bandwidth of the phase-locked loop which filters the direct digital frequency synthesizer (DDS). This lower bandwidth smooths the 512 Hz (corresponding to approximately 1% of the machine momentum acceptance) frequency step-changes from the DDS at the expense of letting more random phase noise from the VCO through. A wideband high dynamic range beam phase detector is now under construction to allow us to carefully check that the RF system is not inducing synchrotron oscillations during the ramp. If any significant amount of coherent synchrotron oscillations remain, a feedback loop will be used to damp them.

We are also in the process of improving the main dipole power supply. Presently the feedback transductor is located in a position where it measures the sum of the current through both the load and the filter capacitor in parallel with the load. The transductor is being moved so that it measures the true load current, and more flexible software is being developed to make ramp programing easier. We are also looking at the measured frequency responses of all the quadrupole power supplies (36), which vary from about 200 to 1000 Hz to see if this is causing a significant tracking problem during the ramps.

During the upcoming year we expect to routinely accelerate from 45 to 287 MeV with respectable efficiencies.

High Intensity Operation

With the high currents (several hundred microamps) obtained with stripping injection and cooled-stacking, we observe coherent dipole synchrotron oscillations, with every nth bunch in phase (n depending upon the RF harmonic number and beam intensity) excited in the low momentum spread electron-cooled beams. We also observe what appears to be a fast transverse instability which causes a beam loss above a certain threshold. In the future, we will build fast dampers, which will act on each bunch individually, to damp the longitudinal instabilities.

1. F. Iselin, The MAD Program, CERN-LEP-TH/85-15.
2. M. Lee, S. Clearwater, E. Gheil, and V. Paxson, in *Proc. of the 1987 IEEE Particle Accelerator Conf.*, edited by Eril R. Lindstron and Louiss S. Taylor, IEEE Cat. No. 87 CH 2387-9, (Washington, DC, 1987), p. 611.

ELECTRON COOLING SYSTEM DEVELOPMENT

T. Ellison, R. Brown, and D. Friesel

Summary

The electron cooling system has now been in operation for about 1 year. During this period the system has been tested over much of its design range, operating with electron beam currents up to 2 A and energies up to 250 keV (the energy required for cooling 459 MeV protons). The system has been used for trouble-free cooling of 44 MeV $^3He^{++}$, as well as proton beams ranging in energy from 45 to 287 MeV (the world's highest energy

electron cooling to date). In addition, a number of cooling tests, which are described below, have been performed with 45 MeV protons.

In the first section below, we discuss the electron collector system which has demonstrated collection efficiencies of up to 100%, $+0/-2$ ppm (parts per million). In the following section, we summarize measurements of the longitudinal drag rate, spanning rest frame electron/proton velocity differences of over three orders of magnitude, and the proton beam longitudinal equilibrium. In the third section, we report on the measured cooled proton beam transverse emittance, and in the final section, on some of the collective beam effects that have been observed with high intensity cooled 45 MeV proton beams.

Electron Collection System

The electron cooling system nominally operates with collection efficiencies of $\geq$ 99.99%. We have, however, demonstrated a technique enabling the system to operate with collection efficiencies of 100% $+0/-2$ ppm (parts per million). The system is quite simple: a horizontal electric field, normal to the longitudinal magnetic guide field in the main solenoid, is used to give the electron beam an $(\mathbf{E} \times \mathbf{B})$ drift to compensate for the centripetal $(\mathbf{R} \times \mathbf{B})$ drift which occurs in the toroids. Using this technique, which is described in more detail elsewhere,[1] any beam reflected from the collector will oscillate in the system, going back to the gun, and then back to the collector where another chance at collection is possible without becoming offset with respect to the primary beam by the toroid centripetal drift, something which occurs when magnetic dipoles are used to correct for the drift.

Longitudinal Cooling Measurements

A. Longitudinal Drag Rate:

The longitudinal drag rate, R_D, (the rate at which the electron beam can change the energy of the proton beam) has been measured in three different ways. The measurement techniques and the theory are discussed in more detail elsewhere[2] and are displayed in Fig. 1. Figure 2 compares this data with data obtained at other electron cooling facilities.

The solid curve in Fig. 1 is the theoretical value for the longitudinal drag rate, using the simple nonmagnetized theory of electron cooling. The data and theory are normalized to an electron current density of 0.2 A/cm^2 (1 Ampere), and for the electron cooling region length equal to the circumference of the storage ring. The electron beam transverse velocity distribution is assumed to be a Maxwellian distribution due to a cathode temperature of 0.11 eV/k (1000°C), where k is Boltzmann's constant. The electron beam longitudinal velocity spread is assumed to be a uniform distribution, the width of which is determined by $\pm$ 4 V cathode potential ripple. The Coulomb logarithm is taken to be a constant, 10.7; the minimum impact parameter ($\sim v^{-2}$) being the classical value determined by the maximum possible momentum transfer, and the maximum impact parameter ($\sim v$) is the Debye shielding length. In both cases, we have taken v to be the rms transverse electron velocity due to the cathode temperature. The electron beam energy is 24.3 keV.

The agreement between the theory and experimental data is quite impressive. The disagreement at high velocity differences can be accounted for the by fact that the model assumes the Coulomb logarithm to be a constant, whereas it actually increases as $3\ln(v_{\|}/v_{e\perp,rms})$, where $v_{\|}$ is the rest frame longitudinal velocity difference between the

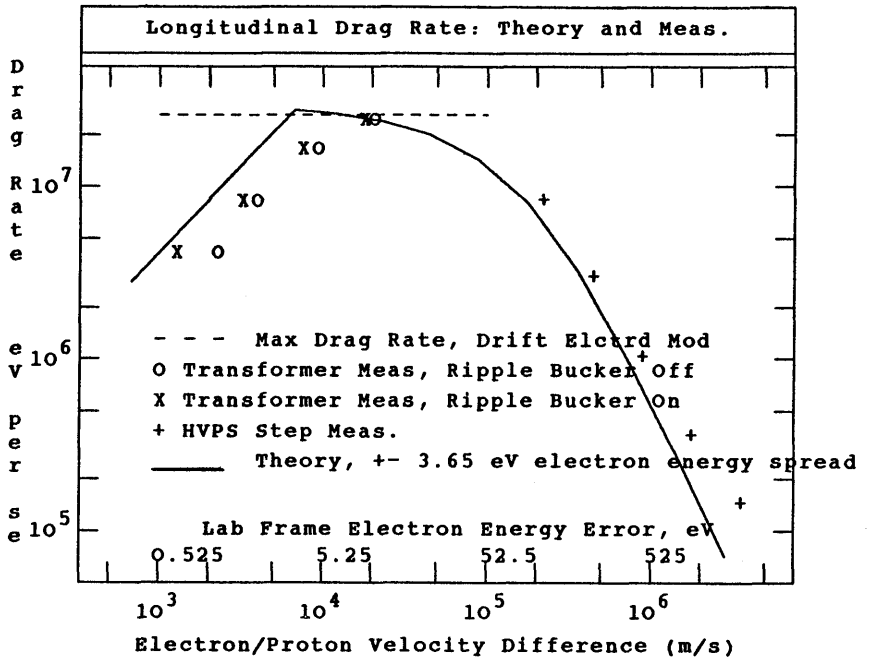

Figure 1. Comparison of longitudinal drag rate measurements with theory. The solid curve is the theory. The horizontal axis is the proton beam longitudinal velocity, in the electron beam rest frame, divided by the electron beam rms transverse velocity (due to the 1000°C cathode temperature).

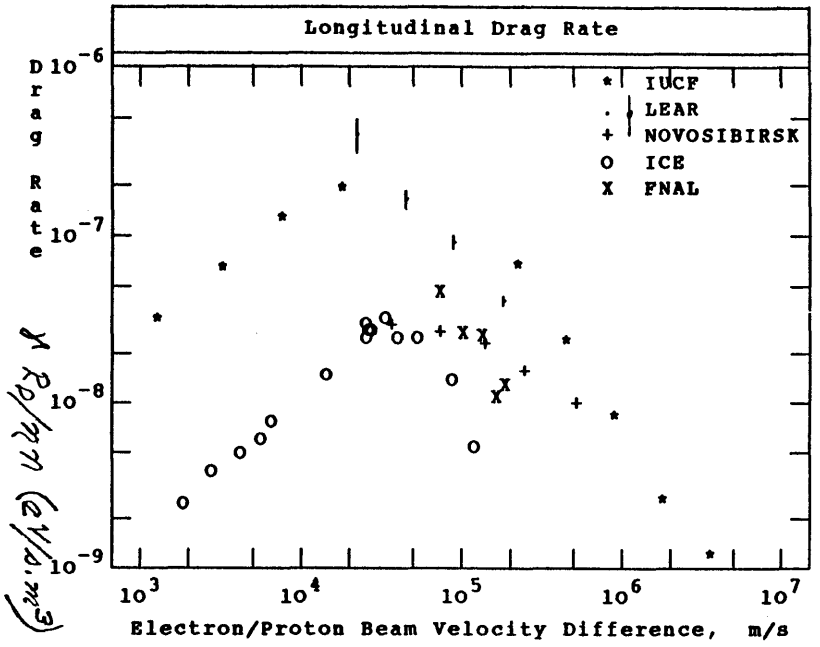

Figure 2. Comparison of longitudinal drag rate data from IUCF with data obtained at other laboratories. The data is normalized to account for different energies, electron densities, and cooling region lengths: the ordinate is $R_D/\gamma\eta n$, where R_D is the measured drag rate, γ the usual relativistic parameter, η the ratio of the cooling length divided by the storage ring circumference, and n the electron density (all lab frame values).

proton and electron beams, and $v_{e\perp,rms}$ is the rms electron transverse velocity due to the cathode temperature.

The disagreement at low longitudinal rest frame proton beam velocities is due to our very approximate model for the electron beam longitudinal velocity distribution. In reality, this velocity distribution is due to a combination of cathode potential ripple, effects due to the electron beam space charge depression, and electron beam intrabeam scattering.[3] It is believed that the electron beam space charge depression is the most important source of the electron beam longitudinal velocity spread.

Studies of the electron beam longitudinal velocity spread were made as a function of electron beam current. The lab frame electron energy spread should remain constant with current if due to the power supply regulation; increase with the 1/6 power of current if primarily due to longitudinal-longitudinal intrabeam scattering; increase with the 1/2 power if due to transverse-longitudinal scattering; and increase linearly with the electron current if primarily due to the electron beam space charge depression. The data from these studies are shown in Fig. 3, where a number of interesting features can easily be observed: Firstly, the electron beam energy spread appears to increase approximately linearly with the electron beam current. (Subsequent tests, which will be reported in the future, confirm that this energy spread is due to the electron beam space charge depression). Secondly, we see that the normalized longitudinal drag rate appears to dramatically increase, above the nonmagnetized theory predictions and measurements shown in Fig. 1, for very small longitudinal velocity differences between the protons and the electrons. Further investigations of the enhancement in the longitudinal drag rate for small longitudinal velocity differences are continuing.

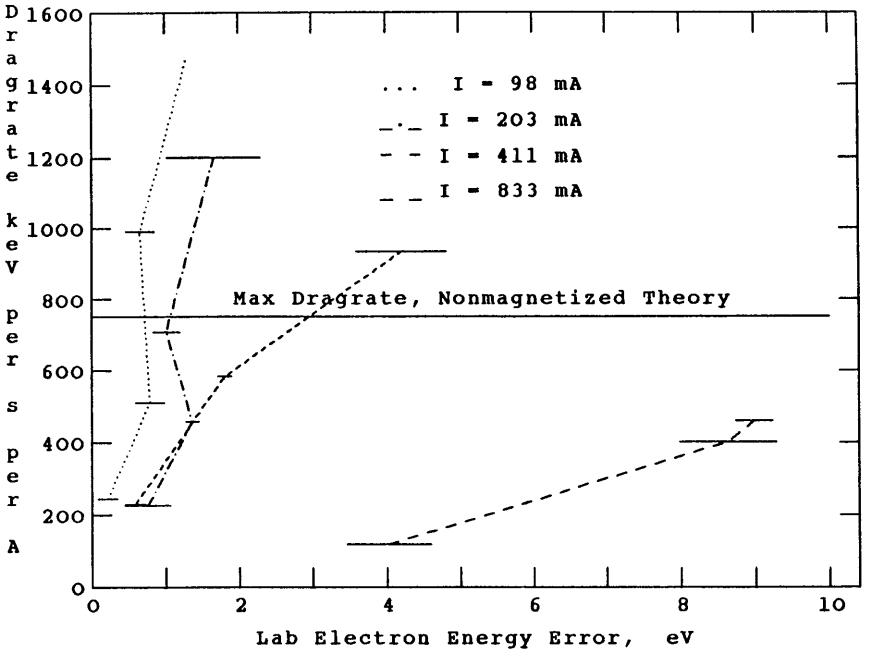

Figure 3. Longitudinal drag rate, normalized to the electron current, as a function of electron energy error for 4 different electron beam currents.

B. Longitudinal proton beam equilibrium:

Video-averaging Schottky signals over a period of time for low intensity ($\approx$1 μA) 45 MeV proton beams yields an effective momentum spread of about 2×10^{-5} (FWHM), corresponding to a 2 keV energy spread. Non-video-averaged Schottky signals have been observed which have frequency spreads of up to 4 times smaller, though these spectra are somewhat suspect since coherent movement of the proton beam momentum can lead to inaccurate measurements of the beam frequency spread. When the beam is RF-bunched, the momentum spreads are generally 3 to 5 times higher. It is not known whether this increase in momentum spread is due entirely to proton intrabeam scattering or to (phase) noise in the RF system.

Equilibrium Proton Transverse Equilibrium

Measurements of the transverse beam size indicate that, for well aligned electron and proton beams in the cooling region, the equilibrium proton beam transverse emittance (1σ) is about 0.05π mm-mrad; this value of emittance translates, in the cooler region, to a beam size of about 1 mm (FWHM) and transverse energy of about 1 eV per plane. These measurements, however, only place an upper limit on the cooled proton beam transverse emittance: the transverse profiles were made with an RF-bunched beam in a region of high dispersion and are also consistent with the RF-bunched beam momentum spread.

Collective Beam Effects

Time domain measurements of the cooled proton beam with a wideband longitudinal pickup show that beams with intensities of greater than 0.1 to 1 μA begin to self-bunch. This bunching can be easily observed on an oscilloscope. Coherent signals in the Schottky signal spectrum extend up to about 200 MHz. The power in an individual "Schottky" band appears to fall off at a rate much faster than the stored beam current for high proton beam currents (where there is a high degree of self-bunching). However, for low currents, the Schottky power falls nearly exponentially with time with an exponential time constant about twice as large as an RF-bunched beam 1/e lifetime.

We have also observed another very interesting effect: at very high proton beam currents ($\geq$ 300 μA), we have seen large coherent signals in the transverse Schottky signal spectra at the upper horizontal sideband (but not the lower). Such a single-sideband signal might be produced if the beam transverse and longitudinal motions were coherently related (e.g., if the beam were self-bunched, and if the betatron motion of particles 90° out of phase longitudinally were also 90° out of phase, one would expect such a single sideband signal).

Figure 4 shows a set of longitudinal Schottky signal spectra from 45 MeV cooled proton beams with currents of (from the bottom) of 0.1, 1, 10 and 100 μA. The beam current for the uppermost trace is unknown. Such behavior is described by Chattopadhyay[4] and has also been observed at the Novosibirsk, LEAR and Heidelberg rings.

Conclusion

The electron cooling system has worked very reliably and presently holds the world's record for the highest energy cooling. The measured longitudinal drag rate is consistent with an effective transverse electron beam temperature equal to that of the cathode. We are

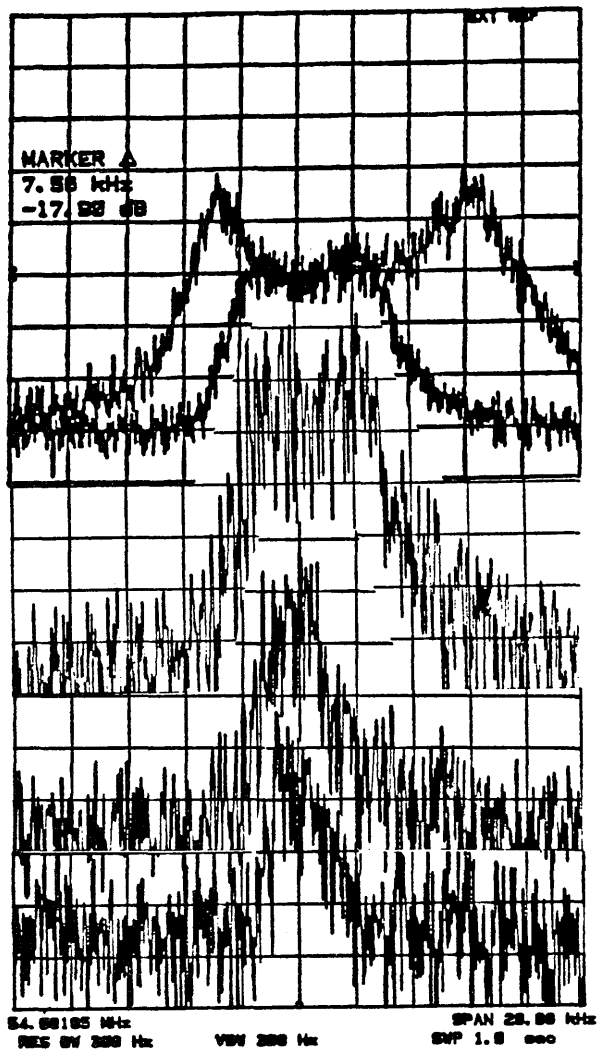

Figure 4. Longitudinal Schottky signal spectra from a coasting 45 MeV electron cooled proton beam. From the bottom, the proton beam current was 0.1, 1, 10, 100 μA; the proton beam current for the uppermost trace is unknown. CF 54.68 MHz (h = 53); 2 kHz/div; 5 dB/ div; RBW = VBW = 300 Hz. The upper two traces were video-averaged 10 times.

now investigating the higher-than-expected longitudinal drag rate which has been observed for small longitudinal electron/proton velocity differences which cannot be accounted for by the nonmagnetized theory of electron cooling. Interesting collective phenomena are observed at high intensities, and thus far, there is no obvious Schottky signal suppression for low intensity beams.

1. Timothy J.P. Ellison, Robert J. Brown, and Brian D. DeVries, The IUCF Electron Cooling System Collector Performance, Nucl. Instr. and Meth., **B40/40**, 864 (1989).
2. Timothy J.P. Ellison, Dennis L. Friesel, and Robert J. Brown, Status and Performance of the IUCF 270 keV Electron Cooling System, Proc. of the 1989 Part. Accel. Conf., Accel. Eng. and Tech. (20-23 March 1989, Chicago, IL). Timothy J.P. Ellison, thesis under preparation, Indiana University Department of Physics.
3. N.S. Dikansky, V.I. Kudelainen, V.A. Lebedev, I.N. Meshkov, V.V. Parkhomchuk, A.A. Sery, A.N. Skrinsky, B.N. Sukhina, Ultimate Possibilities of Electron Cooling, Preprint 88-61, Institute of Nuclear Physics, Novosibirsk (1988).

4. Swapan Chattopadhyay, Some Fundamental Aspect of Fluctuations and Coherence in Charged-Particle Beams in Storage Rings, CERN 84-11, Proton Synchrotron Division (8 Oct. 1984).

NEW NONDESTRUCTIVE BEAM DIAGNOSTICS FOR THE IUCF CYCLOTRON

M. Ball, T.J.P. Ellison, and C.M. Fox

New nondestructive cyclotron beam diagnostic systems which have been developed at IUCF include a beam time of flight system having a kinetic energy resolution of less than $\pm$ 5 $\times$ 10^{-5} (1σ) and improved electronics for our beam phase detector and beam position monitoring system. New beam diagnostics under development include a cyclotron beam turn counter, a new extensive Beam Position Monitor system, and high voltage terminal bunchers.

Beam time-of-flight (TOF) system

Two 7.5 cm length Q-electrodes, separated by 8.515 m, are mounted in a straight section of beam line immediately after the main cyclotron. This system, which is used with pulse-selected beams, measures the relative phase between the RF voltages induced by the beam on the two electrodes using a HP4195A network analyzer. The measurements are made at about 270 MHz at a harmonic of the beam pulse repetition frequency which is not also a harmonic of the cyclotron RF system frequency, making the system absolutely free from RF interference.

A measurement with $\pm$ 0.5° precision at this frequency ($\pm$5 ps), which is easily obtainable, gives an energy resolution of about $\pm$18 keV for a 100 MeV proton beam (about $\pm 1 \times 10^{-4}$ Δp/p). In actual use, with beams with intensities $\geq$80 nA, we can resolve momentum changes 5 times smaller than this. For example, a recent series of 22 cyclotron beam energy measurements taken over a period of 1/2 hour for an 80 nA 135 MeV proton beam had fluctuations with a standard deviation of 5.5 keV ($2 \times 10^{-5}\Delta$ p/p). The high precision of this system is shown in Fig. 1, which is a copy of the network analyzer display which is made available to the operators.

This system is now used as the standard for setting the beam energy for Cooler runs where the precise setting of the beam momentum ($< \pm 2 \times 10^{-4}$) is essential. Besides being extremely precise and repeatable, the system is easy to use. For example, it is not necessary to precisely set slits and adjust the beam position and angle at the entrance and exit of an analyzing magnet in order for this system to give a valid measurement.

Although the precision of this system is extemely high, there is an uncertainty of about 6×10^{-4} (Δp/p) in this system's accuracy. The system calibration was checked by measuring the energy mismatch of the cyclotron beam to the Cooler using Schottky signals and qualitatively looking at how the beam behaves as it is transferred bucket-to-bucket into the Cooler. Here we find that we must add about 52 ps delay as an error term in order to provide the Cooler with an optimal energy 45 MeV beam. This corresponds to an error of about 54 keV ($6 \times 10^{-4}\Delta$p/p). This may be due to an error in measuring the distance